International Journal of Fatigue 159 (2022) 106763

Contents lists available at ScienceDirect

International Journal of Fatigue

journal homepage: www.elsevier.com/locate/ijfatigue

Estimation of weld defects size distributions, rates and probability of detections in fabrication yards using a Bayesian theorem approach

Peyman Amirafshari *, Athanasios Kolios

University of Strathclyde, Department of Naval Architecture, Ocean and Marine Engineering, Glasgow, United Kingdom

ARTICLE INFO

Keywords:
Statistical analysis
Probability of detection (POD)
Bayesian inference
Reliability
Defects
Non-destructive evaluation (NDE)
Engineering Critical Assessment (ECA)

ABSTRACT

Estimation of probability detection curves for non-destructive evaluation (NDE) typically involves the manufacturing of a high number of defect specimens followed by trial NDE and statistical analysis of the data based on the hit/miss approach. This is a time-consuming and costly procedure. Besides, probability of detection (POD) depends on a number of variables, such as human factors (operator), and the testing environment, resulting in a significant mismatch between those POD curves generated in the lab and those in practice.

One application of POD curves is in the quality control of welded joints [1]. Weld quality is often characterised by the number of defects found and their size which is, inevitably, dependent on the POD of the employed NDE. Therefore, a predefined generic POD curve has certain limitations.

In this paper, a method of estimating POD curves based on the Bayesian theorem of conditional probability is presented and its applicability is validated by studying an existing database under both Bayesian and the hit/miss methods. Overall, the POD predicted by the Bayesian theorem is found to be consistent with the commonly used hit/miss model. Finally, the Bayesian model is used to estimate the POD, and the true weld defect size and frequency in two ship manufacturing yards. The estimated weld defect size and frequency models provide valuable information to estimate the fatigue and fracture reliability of ship and offshore structures. It is shown that one of the yards has both better weld quality production and superior NDE detection. This will have a valuable benefit for weld quality control (QC) programmes through saving the testing resources.

1. Introduction

Non-destructive evaluation (NDE) refers to a wide range of technologies used to evaluate characteristics of a component or a system without damaging it. Commonly, a number of other terms has been used to describe these technologies: Non-destructive inspection (NDI), Non-destructive examination (NDE), Non-destructive testing (NDT) and Non-destructive evaluation (NDE). Strictly speaking, these terms refer to deferent meanings, i.e. NDI deals with technicality related to carry out an inspection (method, equipment, phases of examination, etc.), while Non-destructive evaluation (NDE) also considers analysis and interpretation of result. Here, the term Non-destructive evaluation (NDE) is chosen and is used hereafter in this paper [2].

NDE technologies have found extensive application in many sectors including engineering, archaeology, and health care services. In engineering, NDE is widely used in structural integrity management, manufacturing and construction quality control, and forensic engineering.

NDE inspection needs to yield reliable results to serve its intended purpose. The capability of an NDE inspection is commonly quantified by the Probability of Detection (POD) concept. i.e. in any inspection attempt there is a probability that a defect will be detected. Conversely, there is a probability that the defect will remain undetected, and this is referred to as Probability of Non-Detection (POND).

POD is dependent on a number of variables e.g. NDE method, human factors, test environment, and defect size [3-9]. Defect size is frequently considered as an independent variable. In structural integrity assessment, it is often useful to plot detection probability against defect size, which constructs the so-called POD curve. The bigger the flaw sizes the more likely that they are detected. Traditionally, and as shown in Fig. 1, the lower bound (%95 confidence interval) curve is used to predict the largest size that can be missed by inspection.

The above definition of POD is based on the classical interpretation of probability. Frequentistic probability interpretation of POD is that the NDE method can only detect a limited number of defects of a certain size. For instance, an NDE method with 50% POD, misses 50% of the

* Corresponding author.
E-mail address: peyman.afshari@gmail.com (P. Amirafshari).

https://doi.org/10.1016/j.ijfatigue.2022.106763
Received 22 August 2021; Received in revised form 9 December 2021; Accepted 21 January 2022
Available online 24 January 2022

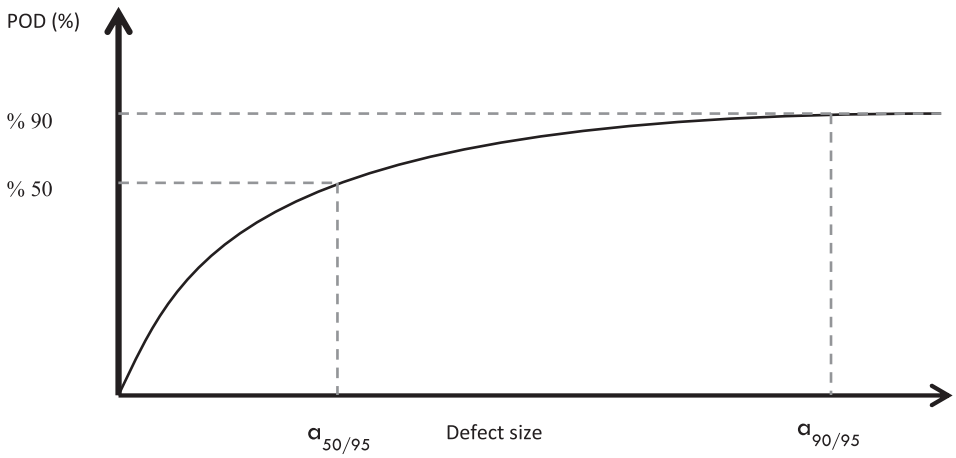

Fig. 1. Schematic lower-bound POD curve of defect.

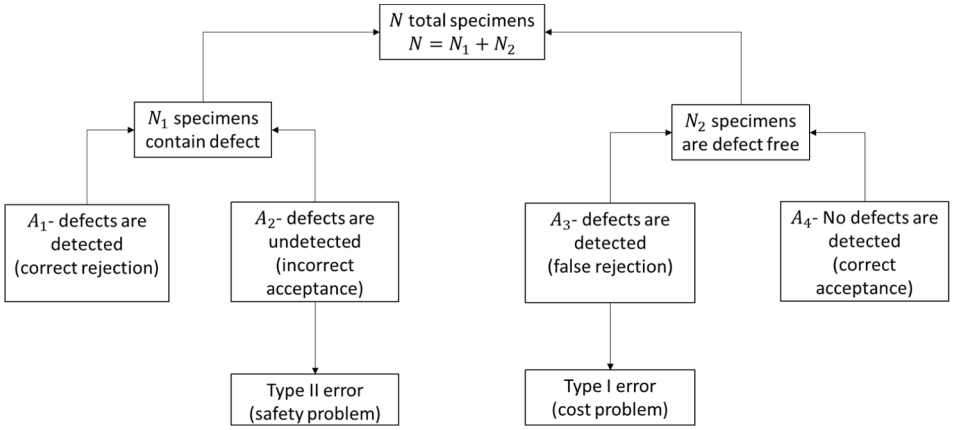

Fig. 2. Possible results of an inspection of n specimens containing A_1 +A_2 defects [10].

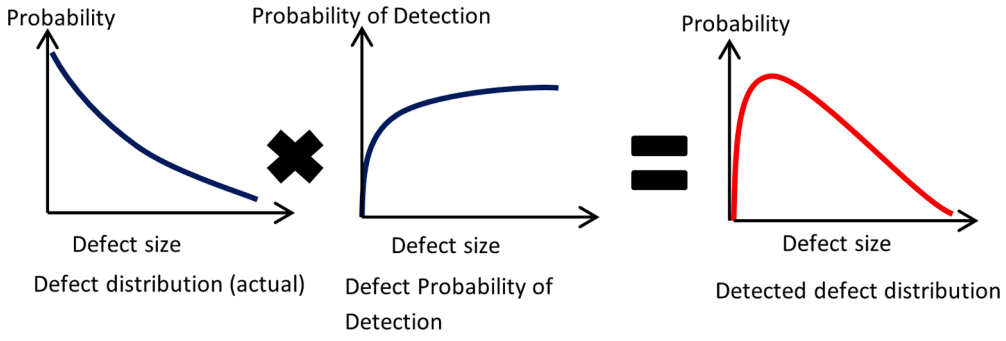

Fig. 3. Relationship between crack size distribution, probability of detection and detected crack size distribution [56].

defects, or if 100 inspection trials are conducted, in about 50 times the defect is missed.

Frequentistic probability is the basis of the experimental approach that has been traditionally used to estimate PODs. As depicted in Fig. 2, the approach involves testing a number of specimens (N); a number of specimens contain pre-existing defects (N_1), and the rest are free from defects (N_2). POD is then the ratio of detected defects (A_1) to defective specimens (N_1), i.e. POD = A_1/ N_1. Based on the outcome of the inspection, other quantities can be defined as: Probability of recognition (POR) = A_4/ N_2, False-call probability (FCP) = A_3/ N_2, and Accuracy of the observer=(A_1 + A_4)/N. These quantities are used to construct the so-called relative operating characteristic (ROC) diagram, which is used to evaluate and optimise the efficiency of the NDE system. In this paper, only POD is discussed.

With the increasing demand for probabilistic integrity assessment of structures, the use of POD curves, which gives the POD over the entire range of defect sizes, has become more common [9,11-13]. The POD curves are used to estimate the actual (detected + undetected) frequency and size distribution of defects. In probabilistic fracture mechanics the actual initial, here-after called "actual", defect size distribution is used as an input, instead of a single deterministic defect size value, [14,15]. Fig. 3 shows the relationship between detected defect size distribution, the POD of defect sizes and the actual defect size distribution (detected + undetected).

Table 1
Parameters that can influence NDE capability [18].

Test object	Defects	NDE technique	Testing condition	NDE Personnel
• Material(s) • Material inhomogeneities and anisotropies • Geometries and geometrical details: Cut-outs, holes, edges, narrow angles • Thicknesses • Surface condition • Coating and insulation	• Type(s) • Size: Length, height, opening/width • Geometrical shape • Orientation • Roughness	• Type and operation principles • Equipment incl. transducers • Equipment characteristic and setting: e.g. frequency • Sensitivity setting • Calibration and functional checks • Preparatory work: cleaning etc. • Reporting format	• Access • Operator positions • Environment type • Temperature • Humidity • Radiation and other hazards • Process and other liquids, including fresh or sea water • Light levels	• Education • Experience • Certification: Type, level • Special training and experience • Motivation • Working hours

Table 2
DNV Parameters for POD curves [9].

NDE method	Description	X0 (mm)	b	50% POD (mm)	90% POD (mm)
Surface NDE	Ground welds or similar good conditions above water	0.4	1.43	0.4	1.9
	Normal working conditions above water	0.45	0.9	0.45	5.17
	Below water and less good working conditions above water	1.16	0.9	1.16	13.3
Visual NDE	Easy access	15.78	1.08	16	121
	Moderate access	37.15	0.95	37	375
	Difficult access	83.03	1.08	83	636
UT		0.41	0.62	0.41	14

Experimental determination of POD is a challenging task since a large number of test trials are required in order to achieve accurate estimates. For example, the ASM Handbook of Non-destructive Evaluation and Quality Control recommends using at least 30 target flaws for hit/miss POD data [16]. Another issue with this approach is that the fabrication of artificial weld defects with dimensions, locations and characteristics that can simulate real weld defects is very difficult to achieve [17].

The issue with the experimental determination of PODs becomes more complex considering that NDE capabilities for weld defects depends on numerous factors. As listed in Table 1, Førli reports a number of parameters that can influence NDE capabilities [18]. In the integrity management of high integrity structures, such as nuclear pressure vessels, every effort is made to achieve the best quality of welds and the highest POD [19]. As a result, only parameters that are difficult to control, e.g. defect orientation, are the most influencing random variables. Therefore, simulation methods, particularly for Ultrasonic Testing, have recently become popular [20,21].

For many ordinary structures, such as ship hulls, offshore oil & gas platforms, wind turbine support structures and bridges, the quality of the weld and the capability of performed NDE varies significantly, even among tests performed on welded joint, from one structure [22]. These types of NDE are often conducted for quality control purposes, [1], and are not meant to provide input for Engineering Critical Assessment (ECA), therefore, consistency of PODs is not usually a goal. However, it would be desirable to quantify the PODs and their variability, which in turn can be used in probabilistic fracture mechanics [9,11-13].

In probabilistic flaw assessment, actual flaw size distribution is more relevant than detected flaw distribution (see Fig. 7), as it accounts for detected and undetected flaws. In practice, first, the flaw size information is recorded, then, using one of the distribution fitting methods a probability density function, which suitably fits the data, is fitted and finally the detection probability of corresponding NDE method is used to calculate the actual flaw size distribution. The key limitation of this procedure is that detection probability depends on and is very sensitive to variables such as human reliability, test environment (shop, laboratory) specimens' geometry, flaw characteristics and material properties [4,5,23]. This would require the acquisition of detection probabilities specific to performed NDE. Such data are not normally available with seasonable confidence.

In this paper, a method based on the Bayesian theorem of conditional probability is presented, which enables the estimation of both POD and actual defect size distributions from the observed data.

2. Existing probabilistic approaches to develop POD curves

2.1. Hit/miss approach

Traditionally, NDE results were treated on a binary basis and whether the defects were detected or not (Accept/Reject). This is referred to as "hit/miss" datasets and was explained above.

The hit/miss dataset is usually analysed using different probabilistic methods to produce a POD(a) function. The detail of the complete theoretical analysis is, however, beyond the scope of this paper. More information can be found in well-cited publications [5,24-26]. A number of different statistical distributions are considered for the best fit among which log-odds (logistic), lognormal, and exponential distributions are the most accepted models [4], and the use of Weibull distribution has also been observed to show a reasonably well behaved model [27]. However, considerations should be given to inspection quality, human errors and multiple uncertain events [3]. Further information can be found in [10]. A number of published works on POD curves have been studied and are briefly reviewed as follows.

The most comprehensive source of POD curves is probably the "Non-destructive Evaluation Data Book" published by the Non-destructive Testing Information Analysis Centre (NTIAC) [2]. The data book contains 411 POD curves for varying test objects based on the log-logistic model, and various materials and defect types. The NDE methods includes, Eddy Current, Ultrasonic Testing, X-radiography Testing, Liquid Penetrant Testing, Magnetic Particle Testing, Visual Testing, and Emerging Testing.

DNVGL-RP-C210_Probabilistic methods for planning of inspection for fatigue cracks in offshore structures, introduces a series of POD curves for Visual inspection, Surface NDE, and Ultrasonic Inspection [9]. The curves provide lower bound values (95% confidence interval). The equation for the curves is as follows:

$$P(x, X_0, b) = 1 - \frac{1}{1 + \left(\frac{x}{X_0}\right)^b} \quad (1)$$

where X_0 and b depend on the inspection scenario with recommended values given in Table 2. X_0 corresponds to the defect size which gives 50% POD.

Visual inspection PODs are given with relation to defect length, as the human eye can only detect the length of a surface breaking defect. Therefore, POD parameters depend on three different access conditions; easy, moderate and difficult access. For example, visual examination of welds with easy access has 90% detection probability of 121 mm long

Table 3
Some of detection probabilities from NTIAC report [2].

	50% POD	90% POD
X-Ray Welds Ground Flushed	4.83 mm	Not Achieved in the test programme
X-Ray Welds with Crowns	5.6 mm	Not Achieved in the test programme

Table 4
Detection probabilities for Radiography testing of Nordtest programme [31].

Radiography testing	Porosity	Solid Inclusion	Incomplete penetration	lack of fusion	cracks
50% POD	1.3 mm	1.01 mm	3.27 mm	0.44 mm	Not Achieved

Table 5
Example of inspection capabilities for sub-surface flaws.

	UT	RT
Minimum size that can be reliably detected, 2a × 2c	3 × 15 mm	1.2 φ pore
Minimum size that can be reliably sized, 2a × 2c	3 × 7 mm	NA
Length sizing accuracy, Δ2c	±10 mm	±2
Through-thickness sizing accuracy, Δ2a	4 mm undersize 1 mm oversizing	NA
Ligament sizing accuracy Δp	±3	NA

defects.

As is presented in Table 2, for surface NDE, POD parameters depend on the conditions of inspection. For UT inspection, the POD curve are described with relation to flaw height [9]. The 90% POD is achieved by a flaw depth (height) of 14 mm.

Kountouris et al. reported probability of detection curves based on a number of independent research projects [7,28-30]. As summarised in Table 3, for welds with crowns, 50% detection probability length is reported to be 5.6 mm, where this POD for weld ground flushed is 4.83 mm. In both cases, 90% detection probability was not achieved in the test programme.

Visser reports a summary of selected parts of the Nordtest NDE programme [31]. The programme took place from 1984 to 1990 in four Scandinavian countries. 730 embedded weld defects and 635 surface defects are reported. Table 4 provides 50% POD values of various defect types for a specific radiography testing as example values.

Annex T of BS7910 provides information on the capability of NDE methods in terms of deterministic values for the minimum size that can be reliably detected and sized [3]. The document also provides sizing errors of the NDE methods. Some example values are given in Table 5. Annex T of BS7910 suggests that radiography testing is not a reliable method for detection of planar defects but is very reliable in detecting porosity type defects [3]. This is consistent with the Nordtest results; however, its philosophy is highly conservative and is generally relevant to short cracks. In reality, as proposed by Dufresne, detection probability using radiography testing increases as the defect length increases, and this is relevant to long cracks that are tolerable by hull structures [32].

2.2. Signal response approach

When signal response vs. flaw size is available (e.g. peak voltage in eddy current, the signal amplitude in UT, the light intensity in fluorescent PT), contrary to the hit/miss model, the data is continuous. It is sometimes called $\hat{a}$ data (i.e. 'a hat data') or 'signal response' data.

For signal response data, much more information is supplied in the signal for analysis than in the hit/miss data. It has been observed in a number of studies that an approximate linear relationship exists between $ln(\hat{a})$ and $ln(a)$ e.g. [5].

$$ln(\hat{a}) = \alpha_1 + \beta_1 ln(a) + \gamma \tag{2}$$

where γ is an error term and is normally distributed with zero mean and constant standard deviation σ_γ. In signal response data, a flaw is regarded as 'detected' if $\hat{a}$ exceeds some predefined threshold $\hat{a}_{th}$, which is decided based on the perceived signal noise [33,34]. The POD(a) function for signal response data (i.e. $ln(\hat{a})$) can be expressed as:

$$POD(a) = Probability(ln(\hat{a}) > ln(\hat{a}_{th})) \tag{3}$$

2.3. Simulation methods

Recently, methods based on computer simulation have become popular [17,20]. In Ultrasonic Testing, POD is related to the likelihood of an overlap between the ultrasonic beam and the defect. The sonic

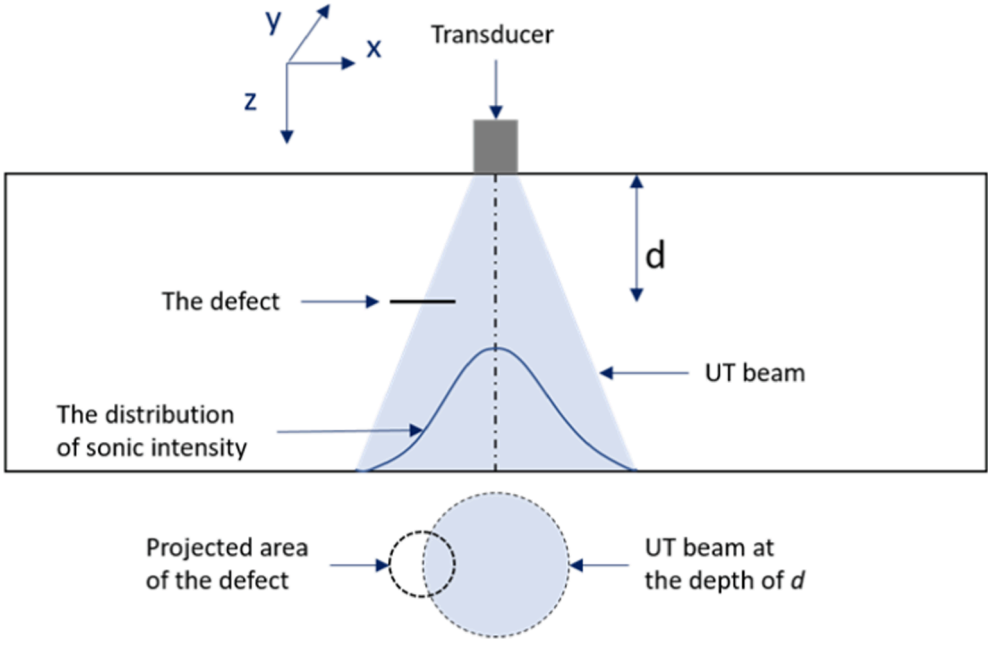

Fig. 4. Illustration showing the interface of a defect and UT beam.

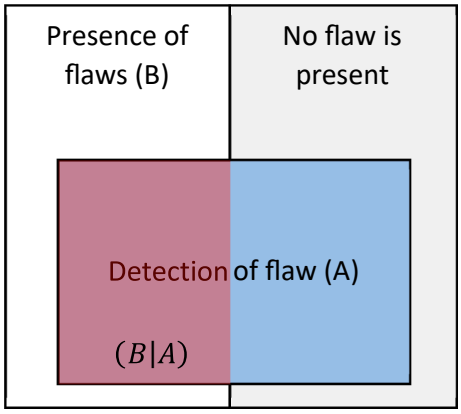

Fig. 5. Diagram of conditional probability for inspection outcome.

	Flaw is present (B)	Flaw is not present $(\overline{B})$
Detection (A)	Correct Detection $P(A\|B)$	False Detection, or detecting other sizes $P(A\|\overline{B})$
No Detection $(\overline{A})$	False Non-Detection $P(\overline{A}\|B)$	Correct Non-Detection $P(\overline{A}\|\overline{B})$

Fig. 6. Conditional probability for inspection outcome table.

intensity of a divergent ultrasonic beam decreases in relation to the centre [21]. Fig. 4 illustrates the sonic intensity distribution as a function of beam divergence. Additionally, there is the attenuation caused by the absorption and dispersion of the wave which is related to the distance d of the defect from the transducer [35,36].

The concept, here, is to calculate the POD by considering the probability distribution of the sonic beam intensity and the probability that the defect area overlaps with the ultrasonic beam. Therefore, factors such as defect orientation, material thickness, defect depth and width can be accounted for.

A Monte Carlo Simulation (MCS) can be used to calculate these probabilities. The estimation of POD with MCS may be achieved by solving the equation below [17]:

$$POD(D) = E[I(x,y)] = \int^{da} \int^{dt} I(x,y) f_{x,y}(x,y) dadt \tag{4}$$

where D is the diameter of the defect (assuming a circular defect); $E[\_]$ is the expected value; x and y are random variables describing the position of the centre of the circular defect; $f_{x,y}(x,y)$ is the joint probability distribution of x and y; da is the distance between two probes and dt is the distance between data acquisitions; $I(x,y)$ is the inspection indicator which assumes 1 for detection and 0 for non-detection. Detection is considered successful when an overlap between the defect and ultrasonic beam happens and the amplitude of the echo produced by the defect is larger than the reference curve.

The MCS solution through the above equation can be obtained as:

$$POD(D) = \sum_{i=1}^{N} \frac{I(x_i, y_i)}{N} \tag{5}$$

where N is the number of simulations.

The commercial POD estimation software, CIVA [37], is a popular software which uses the simulation principle to estimate PODs [20]. The software takes into account the most influential parameters involved during an inspection, concerning the transducer, the geometry and the material in order to optimise the choice of NDE method and minimise the cost of mock-up tests [38].

The main limitation of simulation-based methods is their limited capabilities to consider factors related to NDE personnel and the test environment [39].

3. Methodology

3.1. Bayesian theorem of conditional probabilities

The hit/miss method has its own merits and applications, but the main limitation is its insufficient capability to provide a POD which accounts for influencing factors such as the operator and testing environment. For instance, in quality control of welds, one key measure of weld quality is the recorded defect rate [22], which depends on POD [40]. Variations in the POD results in variations in the estimation of the recorded defect rates, i.e. higher POD results in higher recorded defect rates. Therefore, a pre-established POD curve has a limited use.

An alternative is to adopt a Bayesian approach. Bayesian approaches have been seeing increasing applications in various fields, where probabilistic predictions are of interest, including NDE [41,42]. Here, we derived the detected flaw distribution in terms of POD and actual flaw distribution according to the Bayesian theorem, Eq. (6) [43], and estimated their statistical parameters by fitting the collected data to the detected flaw distribution.

$$P(A|B) = \frac{P(B|A)*P(A)}{P(B)} \tag{6}$$

where $P(A|B)$ is a conditional probability and is the likelihood of event A occurring given B is true. Here, $P(A|B)$ is taken as the probability of a flaw (of a certain size) being present given the flaw (of a certain size) is detected. $P(B|A)$ is a conditional probability and is the likelihood of event A occurring given B is true. $P(B|A)$ is the probability of detecting a flaw given a flaw of a certain size is present. $P(A)$ and $P(B)$ are the probabilities of observing A and B independently. $P(A)$ is the occurrence probability of a flaw (of a certain size). $P(B)$ is the probability of detecting a flaw of any size, the concept is depicted in Fig. 5 and Fig. 6.

The concept can be applied to probability distributions, as well [44]. Therefore, $P(A|B)$ becomes the detected flaw distribution, and $P(B|A)$ becomes the POD curve. $P(A)$ is the actual defect distribution (detected and undetected), and $P(B)$ is the integral of POD $\times$ $P(A)$, i.e. the sum of probabilities of each defect size times their probabilities of detection.

The task here, is to derive the detected defect distribution ($P(A|B)$) equation in terms of actual defect distribution ($P(A)$) and POD curve ($P(B|A)$), which can be achieved simply by using Eq. (6). Then, by fitting the detected defect size data into $P(A|B)$, the parameters for all three distributions can be estimated.

In general, the POD curve follows a monotonic incremental distribution function, although some cases of non-monotonic POD curves can be found in the literature, e.g. as in [26]. Cumulative log-logistic, lognormal, and exponential distributions are the most widely accepted models [4]. Although simplistic exponential distribution provides a less representative fit compared to log-odds (logistic) and lognormal, it still represents an adequate form.

For fabrication weld defects, the size distribution can be appropriately represented with an exponential density function [4]. It is expected

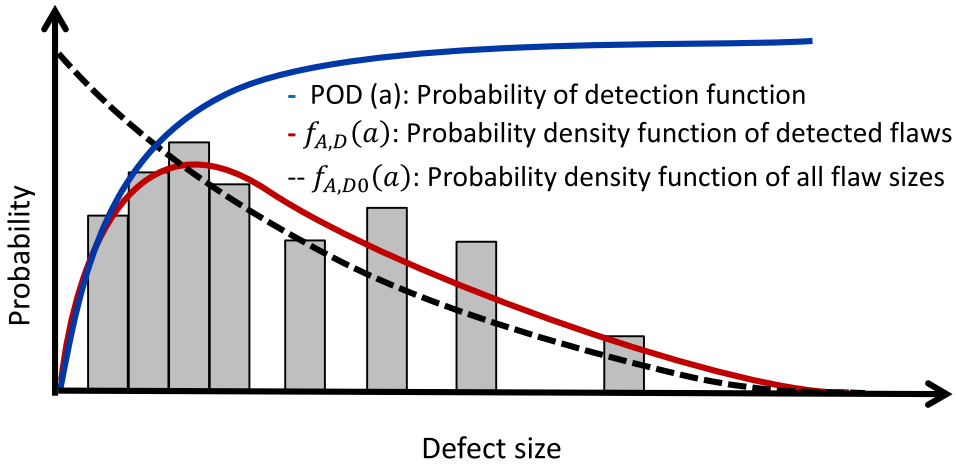

Fig. 7. Schematic description of defect size distributions [56].

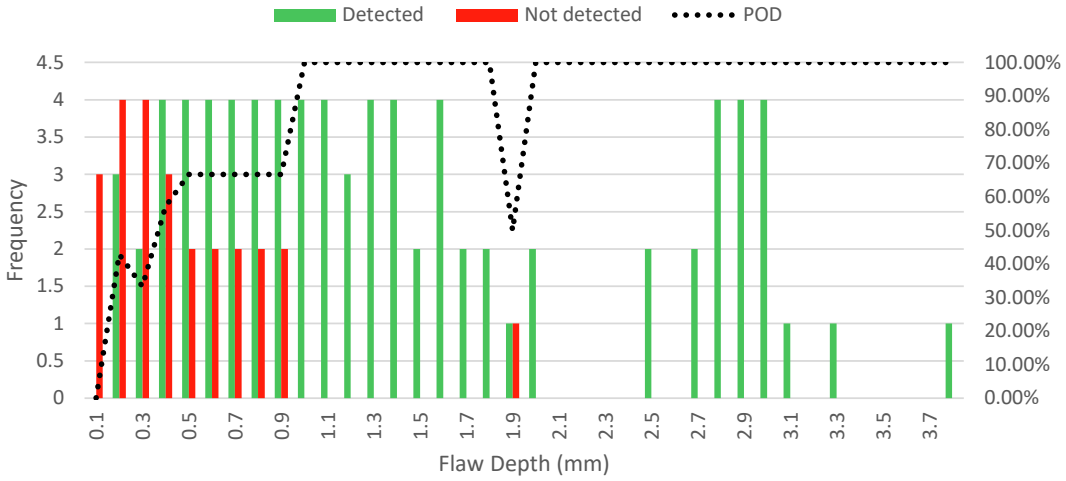

Fig. 8. Histogram of hit/ miss data.

that there would be a large number of small defects, and a much lower number of large defects [45-48].

The exponential distribution is a convenient choice of distribution from a data fitting perspective, since it is only defined by one parameter. The exponential probability function of flaw size (a) with mean flaw size λ_0 is described by Equation (7):

$$f_{A0}(a) = \frac{1}{\lambda_0} e^{-a/\lambda_0} \tag{7}$$

The POD curve is approximated by the cumulative exponential function with crack size parameter λ [49].

$$POD(a) = 1 - e^{-a/\lambda} \tag{8}$$

The probability of detecting a flaw of any size can then be calculated as follows:

$$P_D = \int_0^\infty POD(a) f_{A0}(a) da \tag{9}$$

The probability density of detected flaws of size a is:

$$f_{A,D}(a) = \frac{POD(a) f_{A0}(a)}{P_D} \tag{10}$$

Note: the division by the integral term ensures that the area under the probability density curve equals 1. This is also called the marginal function [50].

The probability density of defects at inspection locations that are not detected is:

$$f_{A,ND}(a) = f_A(a)(1 - P_D(a)) \Big/ \left(\int_0^\infty f_{A0}(a)(1 - P_D(a)) da \right) \tag{11}$$

where $\int_0^\infty f_{A0}(a)(1 - P_D(a)) da$ is the probability of an undetected defect at an inspected location.

The POD curve, detected defect distribution and fabriction defect distribution (detected + undetected) are illustrated in Fig. 7.

When more than one inspection trials is conducted on the test specimen(s), the probability distribution on undetected defects from previous inspection (Eq. (10)) can be treated as the probability density function of all the flaws in the current inspection. Therefore, a new set of parameters, including for the POD, may be estimated.

$$f_{A,D}^{i+1}(a) = \frac{POD^{i+1}(a) f_{A,ND}^{i}(a)}{P_D^{i+1}} \tag{12}$$

Moan et al examined crack data from more than 4,000 in-service NDE inspected welded joints of offshore jacket structures using Magnetic Particle Inspection (MPI) by fitting the data into the model described in Eq. (10) and Eq. (11), and the estimated POD curves [49]. They used data from consecutive inspection trials. They adopted the method of moments (MOM) fitting technique to estimate λ_0, and λ.

Table 6
Summary of statistical data fitting to candidate probability distributions.

Flaws	Dist. Type	Dist. Parameters		Log Likelihood
Detected	Gamma	a = 2.08	b = 0.07	−102.52
	Weibull	Scale = 1.62	Shape = 1.55	−102.58
	Lognormal	μ= 0.12	σ = 0.78	−105.47
Detected + undetected	Gamma	a = 1.45	b = 0.84	−122.80
	Weibull	Scale = 1.3	Shape = 1.25	−122.85
	Exponential	Mean = 1.22		−126.8
	Lognormal	μ= −0.187	σ = 0.98	−127.8

3.2. Proof of concept

Although the application Bayesian conditional method is a well-established, [49,51,52] method, since this paper intends to study weld defect rate and size statistics using this method instead of commonly adopted hit/miss method, first, adequacy of the Bayesian method is demonstrated by estimation of POD curves using the Bayesian conditional probability theorem and the hit/miss method, here, then the method is applied to fabrication defect size data of two ship yards in the analysis section. In this section, a pre-existing dataset from literature is used to estimate relevant curves (i.e. POD, detected defect sizes, and 'detected + undetected' defect sizes) using both methods.

3.2.1. Data acquisition and distribution fitting

The data reported by Georgiou [5] were used. The analysed dataset is given in the Appendix section. Georgiou, [5], plotted the NDE defect depth from the NTIAC data book [2]. The NDE dataset includes 105 data point flaws in aluminium flat panels with thicknesses of 1.5 mm and 5.6 mm. Overall, 81 flaws were detected, and 25 flaws remained undetected. Fig. 8 shows the frequency histogram of detected and undetected flaws. It can be observed that 50% POD is achieved at 0.4 mm and, apart from the data point at 1.9 mm, 100% is achieved at 1.0 mm.

Detected flaw size data and detected + undetected flaw size data were fitted into candidate distributions using the maximum likelihood estimate (MLE) method. MLE is the most commonly used method of distribution fitting compared to other commonly used methods such as method of moments (MOM) and method of percentiles (MOP), due to its superior statistical properties, namely, consistency, asymptotic normality, asymptotic efficiency, and its invariance. Further information can be found in [53].

The gamma, Weibull and lognormal distributions showed the best fit to both set of data. The relative goodness of fit was assessed by comparing the corresponding log likelihood values, as given in Table 6. For detected + undetected data, the exponential distribution showed a slightly better fit than the lognormal distribution. Although, the gamma has given a higher log likelihood value than Weibull, the difference is very small.

Decision on the choice of the probability distribution function which best represents the data is not always purely based on statistical properties (e.g. goodness-of-fit measures). In practice, the nature of the phenomena underlying the analysed data, the applications of the data, and experts' elicitation often play a significant role. For instance, size data (i.e. defect length, width, depth) always assume positive values; therefore distributions that allow negative quantities should be ruled out. An example of the effect of the application of data is when defect size data are used for ECA; larger defect sizes are often those that cause failure in a structure, therefore distributions that provide better fits to the tail of the data should be used. In probabilistic ECA, the critical crack sizes, when considered with other probabilistic parameters [54,55], may be located further from the tail of the distribution towards the median, due to their higher probability of occurrence [56,57].

Although a visual assessment of fitted distributions and data without quantitative metrics is scientifically and methodologically not acceptable, it is often insightful, particularly for ensuring that the fits adequately describe the data. Fig. 9 shows the detected flaw probability density histogram and fitted distributions. It can be observed that Weibull and gamma distributions better describe the general shape of the histogram of the data compared to the lognormal distribution. However, one should be careful when doing a visual assessment of the histogram of the data, since the shape will depend on the choice of bin width. Alternatively, a better observation can be made by plotting the cumulative probabilities of data points and the fitted distributions, as shown in Fig. 10. It can be observed that all three distributions show reasonably good fits. Contrary to the Weibull and gamma, the lognormal distribution overestimated the data at the left side of the data range and underestimated the data at the right side of the data range.

Fig. 11 shows the detected + undetected flaw probability density histogram and fitted distributions. It can be observed that Weibull and gamma distributions better describe the general shape of the histogram of the data compared to the lognormal and exponential distributions. Fabrication weld defects can be as small as close to zero (microscopic surface defects), therefore an exponential distribution is considered to be a better representative of such defects [4,8,58-60]. Note that flaws in the dataset, analysed here, are artificial flaws, i.e. generated for testing

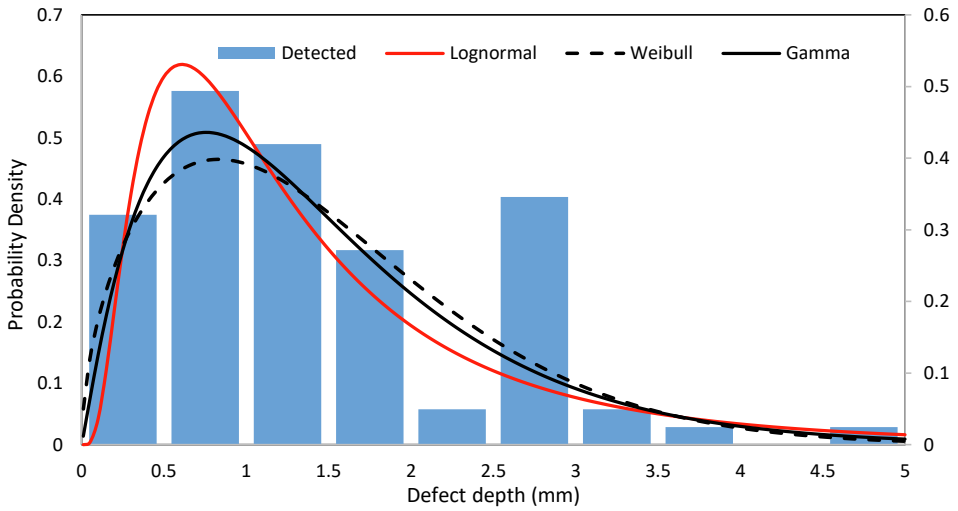

Fig. 9. Detected flaw probability density histogram and fitted distributions.

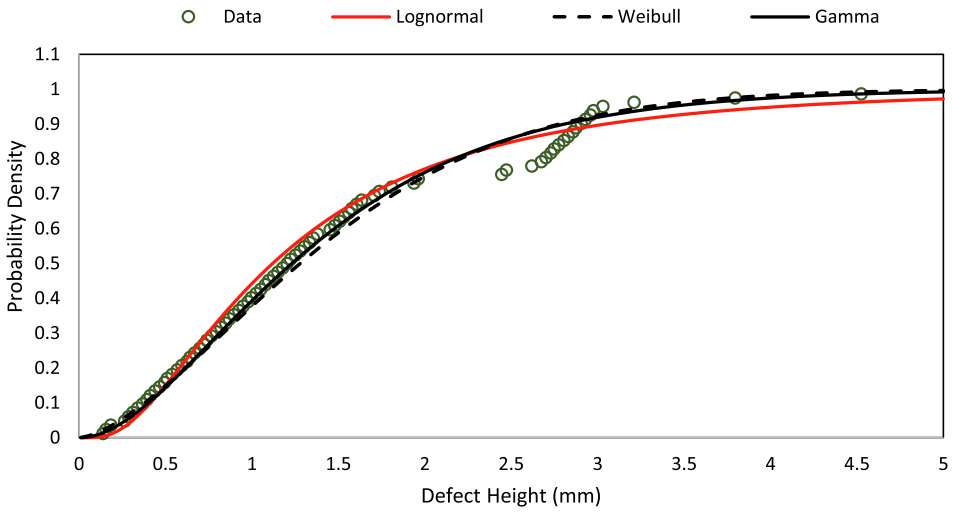

Fig. 10. Detected flaw cumulative probabilities of data points and fitted cumulative density functions.

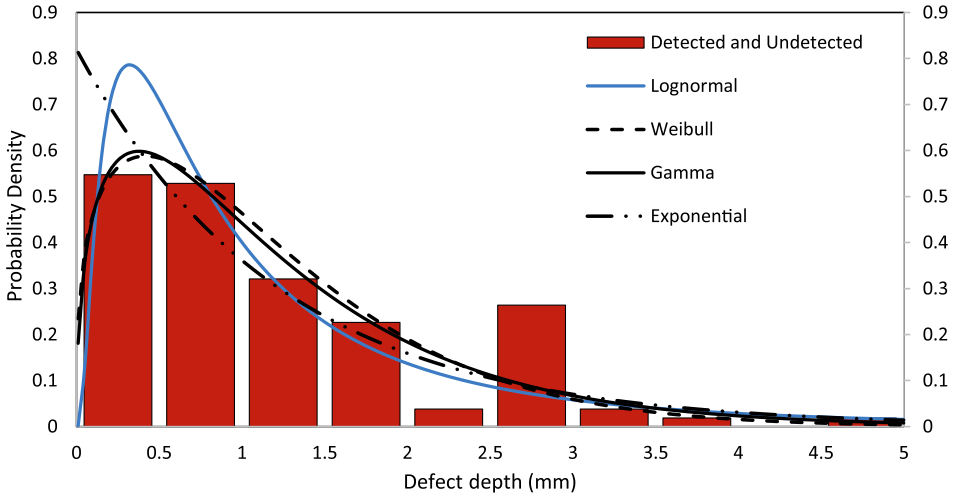

Fig. 11. Detected + undetected flaw probability density histogram and fitted distributions.

and their frequency and sizes are not strictly representative of weld defects.

3.2.2. *Estimation using Bayesian theorem*

Detected, detected + untdetcted size distributions were estimated using the Bayesian method and fitting only the observed (detected) data to Equation (10) using MLE method. The corresponding equations are plotted in Fig. 12 and Fig. 13. The estimated parameters are summarised in Table 7 and the goodness of fit results are given in, Table 8. The parameters were also estimated based on the hit/miss approach and using MLE and Least Square Estimate (LSE) by fitting detected + undetected flaw sizes to Equation (7) and POD values to Equation (8); the relevant results are summarised in Table 7 and 8.

As it can be observed from Table 7, and Table 8, and Fig. 14 and Fig. 15, the Bayesian estimate is less conservative in estimation of the detected + undetected distribution, but the its POD is very close to the POD estimated by the hit/miss approach.

It can be understood from the goodness-of-fit results given in Table 8 that the Bayesian method estimates POD very well and the detected + undetected distribution is reasonably close to the actual distribution estimated with the hit/miss method.

Overall, the Bayesian approach provides particularly good estimates considering that, contrary to the hit/miss model, there is no input from undetected defects to the Bayesian method, as it only uses a presumed distribution type.

This is very valuable in view of the practical implication of the model. Consider, for example, the NDE inspection of newbuilding ship hull structures and offshore support structures for wind turbines and oil rigs at fabrication yards. The NDE inspection is performed on a sampling basis to assess the general quality of welds [22,61]. The measure of quality for the Quality Control (QC) team is the defect rate and size [22,45,62]. As pointed out earlier, these quantities are dependent on the POD of the employed NDE. It is normal in fabrication yards for the NDE conditions (e.g. personnel, test environment) to vary during fabrication time and among different workshops of the yard. Therefore, one issue that is always raised is whether the variation in defect rate and size is due to variation in welding quality or the variation in NDE capability [61]. While assessment of the variation in NDE capability using hit/miss approach will not be cost-effective and, perhaps, not representative of actual NDEs, the Bayesian method, outlined above, gives the means for such assessments without any additional testing costs and time intakes.

4. Analysis

As outlined in the introduction and methodology sections the detected + undetected distribution of weld defects is a key input for

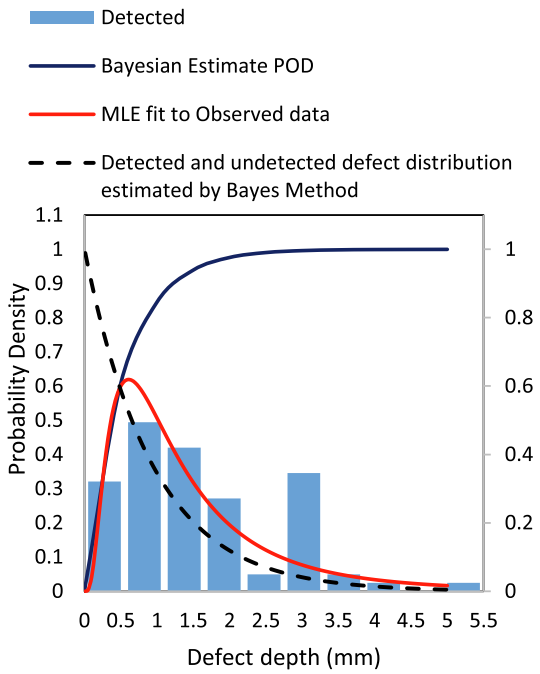

Fig. 12. Detected data histogram & estimated functions.

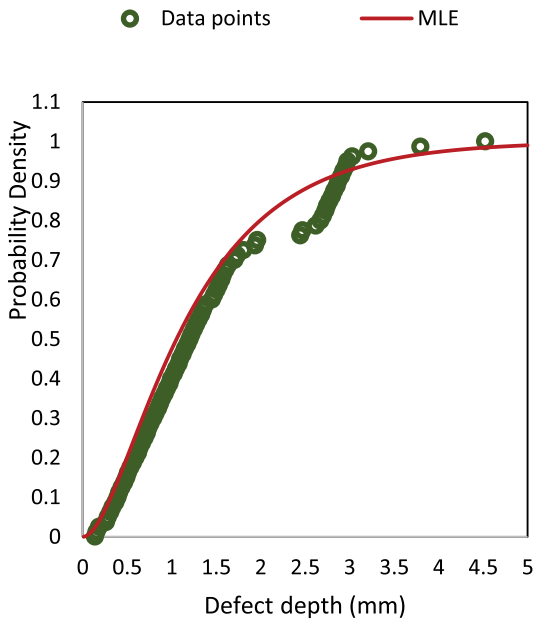

Fig. 13. Cumulative distribution fit to observed data.

Table 7
Summary of distributions parameters estimations.

Method	Detected + undetected dist. λ_0 (Mean defect size mm)	POD λ (Mean detection size mm)
Bayesian	0.94	0.536
Hit/Miss	1.21	0.515

probabilistic ECA, and corresponding defect rates are crucial measures to assess the quality of the welding process, respectively. The severity of defects types from a fatigue failure point of view depends on the type of those defects, planar defect such as cracks and LOP/LOF are much more damaging than nonplanar defects such as cavities and solid inclusions

Table 8
Goodness-of-fit results.

	Hit/Miss	Bayesian
Goodness of fit measure	Log Likelihood	
Detected flaws	−102.57	−103.248
Detected + Undetected	−126.807	−130.662
Goodness of fit measures	Sum of Squared Errors (SSE), R-Squared	
POD	SSE = 0.3608, R-Squared = 0.8154	SSE = 0.3617, R-Squared = 0.8150

[63]. Here, the Bayesian method was used to estimate relevant distributions and defect rates for data from two fabrication yards.

Amirafshari et al. analysed weld defect data collected from two fabrication yards and reported detected defect types, lengths and rates [64]. The welds included butt welded joints connecting shipbuilding steel grade AH36 with thicknesses ranging between 5 and 25 mm. The welding processes were Flux Cored Arc Welding (FCAW), Submerged Arc Welding (SAW), and Hybrid Laser Arc Welding (HLAW). The defects were detected using Radiography Testing (RT). Using the approach outlined in the Methodology section, the dataset reported by Amirafshari., [64], was used to estimate mean actual defect length, λ_0, and mean detection length, λ. λ_0 is the parameter for exponential distribution, as given by Equation (7), which describes actual defect length distribution and λ is the parameter for cumulative exponential distribution which describes the POD curve, as given by Equation (8). The data were fitted into Equation (10) using the MLE method. Amirafshari et al. showed that the reported defect distributions show bi-modality, [64], indicating that the defects are produced by two phenomena. The first are due to the natural randomness in defect length which can be described by the exponential distribution and second are those larger defects produced by especial causes and therefore where, visually identified and excluded from analysis here. The summary of the parameters estimation results is given in Table 9.

5. Results and discussion

POD curves for various defect types, actual (detected + undetected) defect length probability distributions, and undetected defect length distributions are plotted and compared in Figs. 16–21 and Figs. 22–29, respectively. Total Probability of Detections (PDs) and Total Probability of non-Detection (PnDs) using Equation (9) are summarised in Table 10. Then, the actual defect rates (by considering the probability of non-detection) were estimated by dividing the defect rates by corresponding PDs. Recoded and actual defect rates are given in Table 11 and Illustrated in Fig. 30 and Fig. 31.

5.1. PODs

Fig. 16 and Fig. 17 show POD curves for Yards 1 and 2, respectively. It can be observed that in both yards the LOP/LOF have highest detection probability, followed by cavity defects and solid inclusions. The PODs for crack type defects are distinctly low compared to the other defect types. This is consistent with what was outlined in Section 2, “Existing probabilistic approaches to develop POD curves”, regarding RT being considered unreliable for detecting planar flaws and very reliable in detecting nonplanar flaws. Although, LOP and LOF defects are typically and prudently categorised as planar flaws for ECA, they may be detected far easier than cracks due to their bigger width; particularly, as shown in Table 4, LOF defects have a substantially high POD using RT. The majority of analysed LOP/LOF defects from the dataset are LOF, i.e. among 111 LOP/LOF defects from yard 1 only 14 are LOPs and the rest, 97, are LOFs. In yard 2 data set 25 are LOFs and 8 are LOPs [64], therefore the high POD observed is likely to be due to LOF

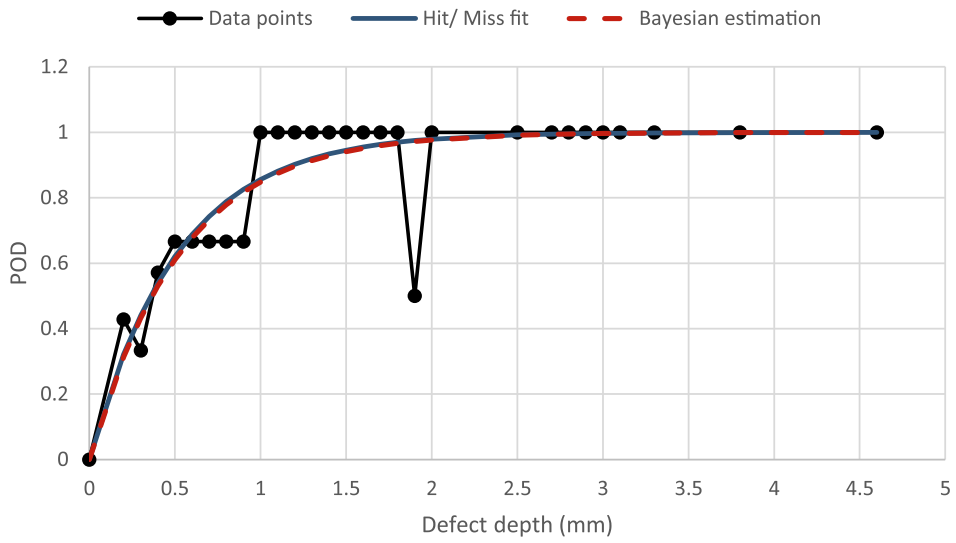

Fig. 14. POD curve estimation using Bayesian method versus the hit/miss method.

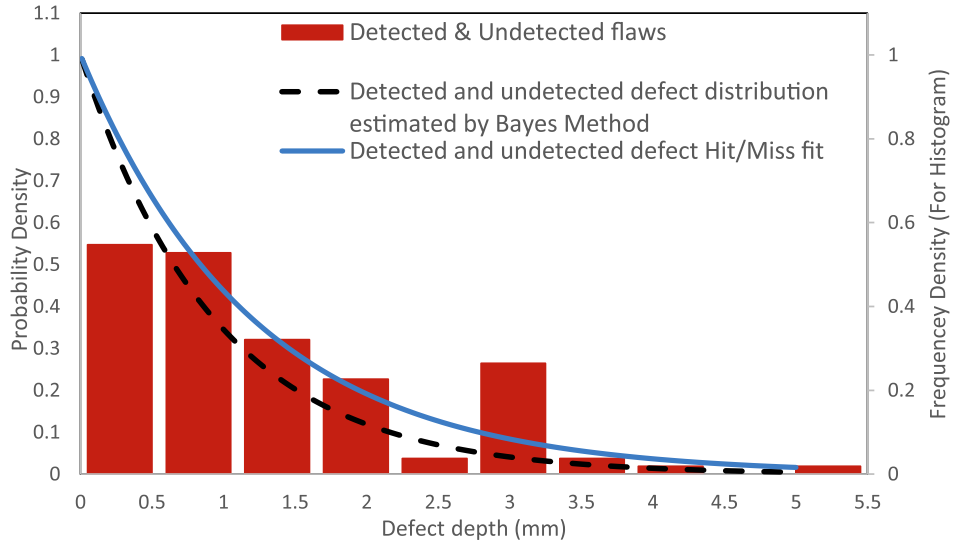

Fig. 15. Detected + undetected data histogram and the estimated functions.

Table 9
Actual defect size distribution parameters (λ_0) and POD curve parameters (λ).

Defect Type	Yard 1		Yard 2		Comments
	λ_0	λ	λ_0	λ	
Crack	13.77	43.28	15.14	23.2	Defects above 120 mm excluded
LOP/LOF	62.32	14.68	80	2.64	Defects above 400 mm excluded
Cavity	41	15	38	8.1	Defects above 300 mm excluded
Solid Inclusion	69.27	32.6	56	10	Defects above 300 mm excluded

defects dominating detected LOF/LOP defects.

Figs. 18–21 compare various PODs of the two yards. It is evident that Yard 2 has better NDE quality as its PODs are higher than those of Yard 1. This is an important revelation as it is not readily possible to determine if one yard is producing a lower quality weld, i.e. bigger and more defects, or it has better NDE capabilities, i.e. the NDE technicians can interoperate RT film better, by just considering the detected defect size

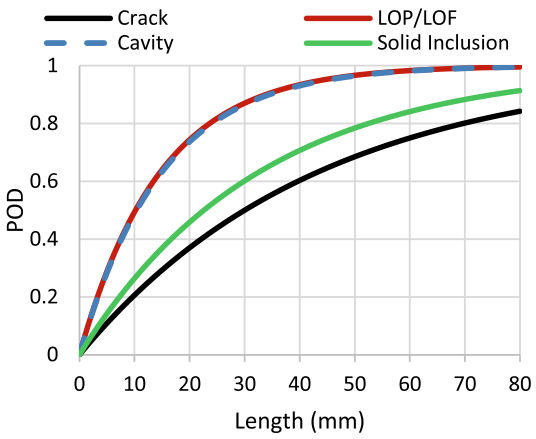

Fig. 16. Estimated POD curves for Yard 1.

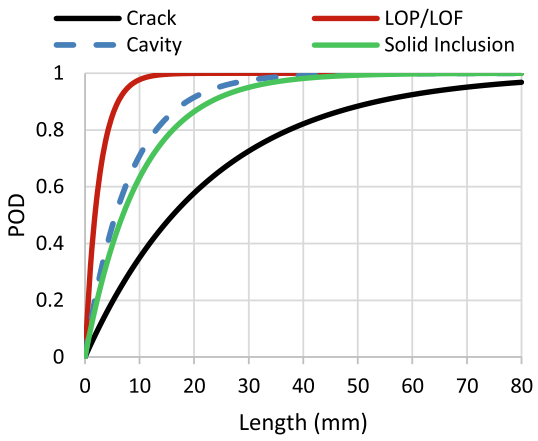

Fig. 17. Estimated POD curves for Yard 2.

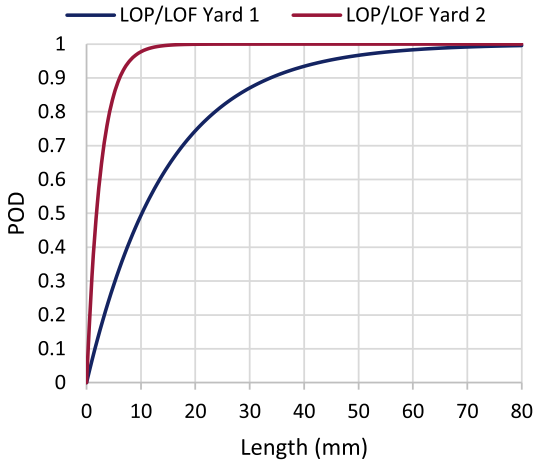

Fig. 18. Estimated POD curves for LOP/LOF defects.

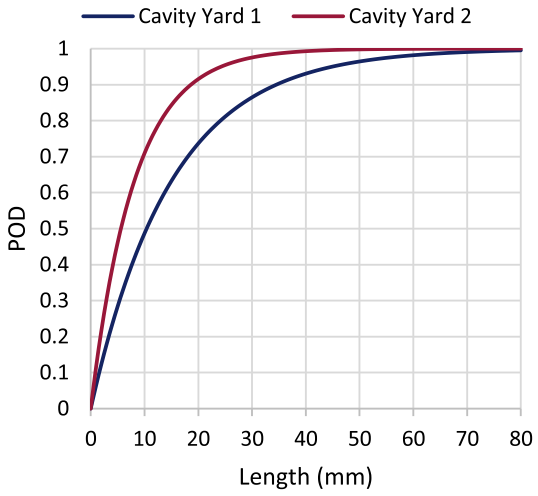

Fig. 19. Estimated POD curves for Cavity defects.

information and PODs need to be estimated.

5.2. Defect size distributions

Actual defect length distributions are plotted in Figs. 22–27 using the λ_0 values given in Table 9. The length distributions of undetected defects

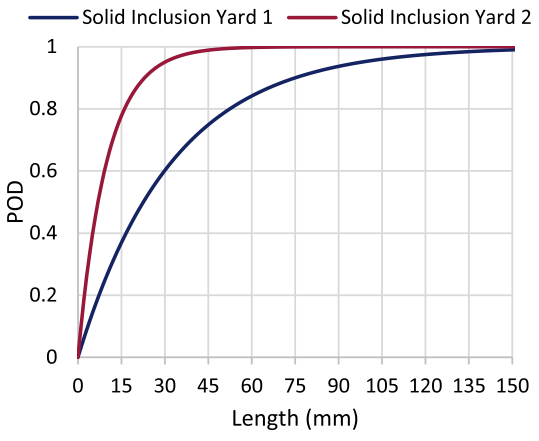

Fig. 20. Estimated POD curves for Solid Inclusions defects.

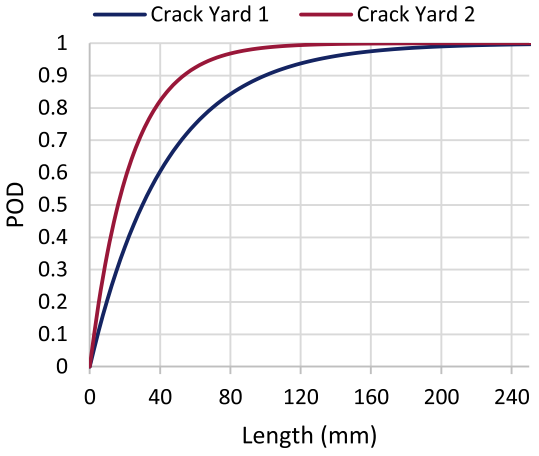

Fig. 21. Estimated POD curves for Crack type defects.

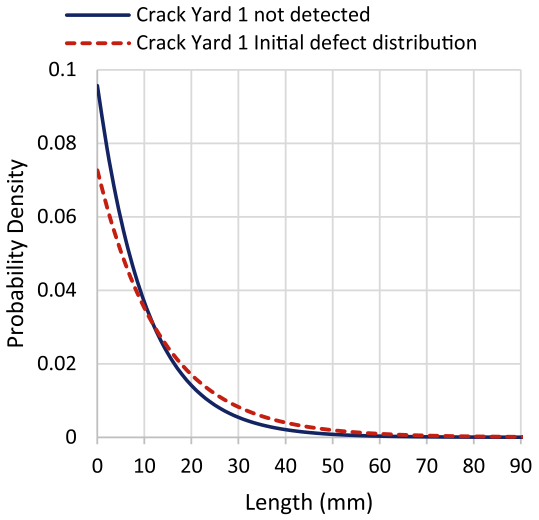

Fig. 22. Not-detected Crack size and Actual crack size (detected + not detected) distributions for Yard 1.

are also plotted using Equation (11) by incorporating the POD curve and actual defect length distribution simultaneously. When all weldments of a structure are inspected, the distribution of not detected defects are representative of defects present in a newbuilt structure, but, when only a number of selected weldments are inspected (partial inspection) [22],

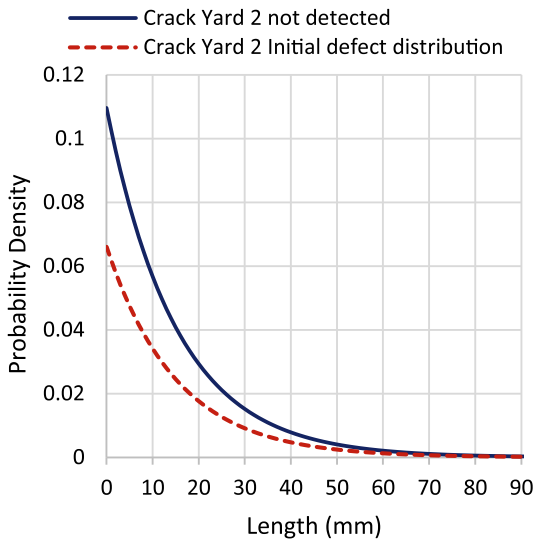

Fig. 23. Not-detected Crack size and Actual crack size (detected + not detected) distributions for Yard 2.

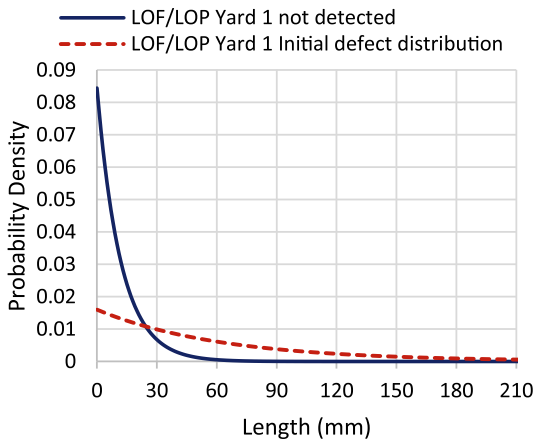

Fig. 24. LOF/LOP Not-detected and Actual size (detected + not detected) distributions for Yard 1.

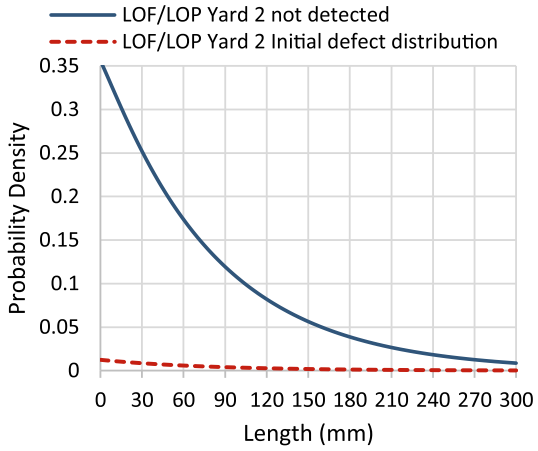

Fig. 25. LOF/LOP Not-detected and Actual size (detected + not detected) distributions for Yard 2.

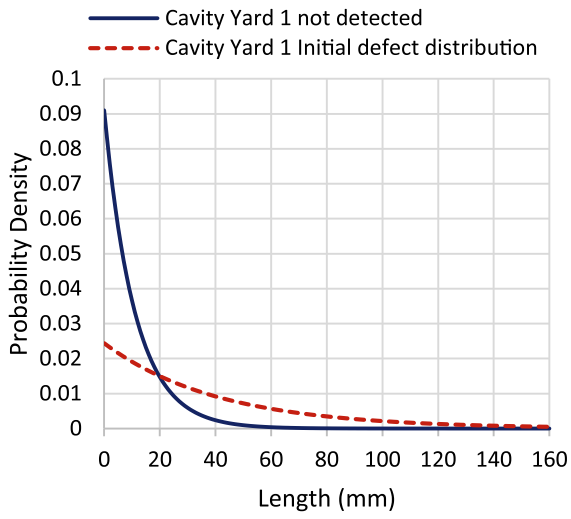

Fig. 26. Cavity Not-detected and Actual size (detected + not detected) distributions for Yard 1.

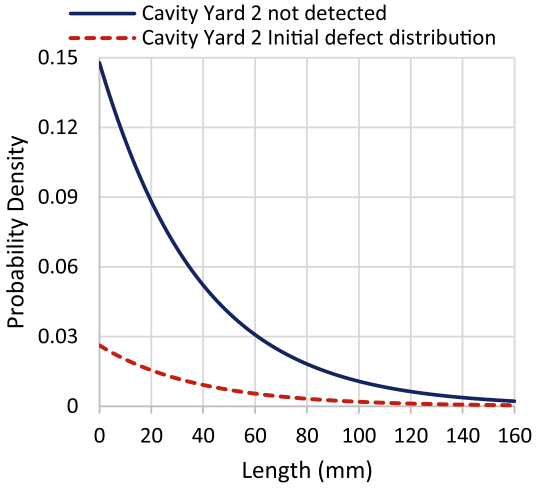

Fig. 27. LOF/LOP Not-detected size and Actual size (detected + not detected) distributions for Yard 2.

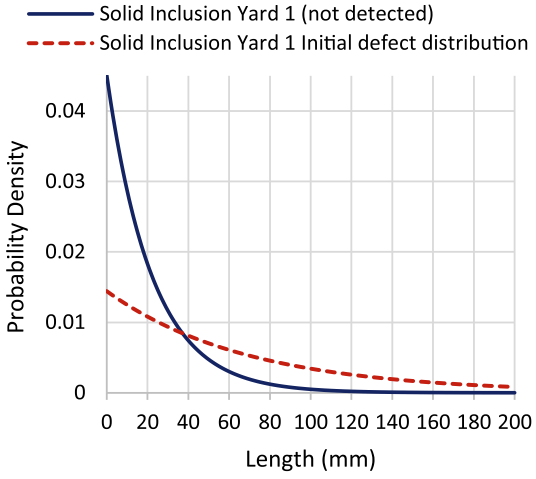

Fig. 28. Solid Inclusions Not-detected and Actual size (detected + not detected) distributions for Yard 1.

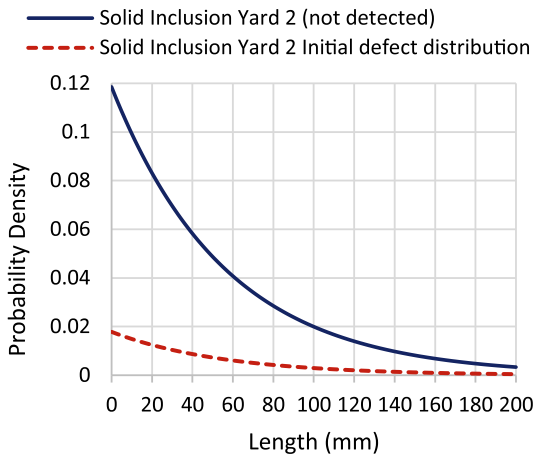

Fig. 29. Solid Inclusions Not-detected and Actual size (detected + not detected) distributions for Yard 2.

Table 10
Total Probability of Detection (PD) and Probability of non-Detection (PnD).

Defect Type	Yard 1		Yard 2	
	PD	PnD	PD	PnD
Crack	0.24	0.76	0.4	0.6
LOP/LOF	0.81	0.19	0.966	0.034
Cavity	0.732	0.268	0.824	0.176
Solid Inclusion	0.68	0.32	0.85	0.15

the actual defect size distribution is applicable. The distributions of cracks, which are the most damaging defect type, can be used in a probabilistic ECA approach to estimate the reliability of the structure [55,56]. As can be observed from Fig. 22 and Fig. 23 the actual defect distributions and the undetected distribution are very close, indicating that RT inspection is not likely to significantly improve the structural reliability.

The total probability of detections (PDs) which mean the probability of finding any defect size given the actual defect size distributions and PODs were estimated using Equation (9) and the results are given in Table 10. The probability of non-detections (PnDs), probability of not finding any defect of any size, is also calculated simply by subtracting 1 from PD.

5.3. Defect rates

The defect rates are often used as a quality control tool at fabrication plants and yards [22]. They also directly influence the reliability of a structure containing weld defects [45,55,56]. The defects recorded rates are strongly dependent on the chosen NDE method, particularly, their PODs: The higher the POD, the higher the recorded defect rate for the same actual defect size distribution. This often encourages fabrication yards to employ NDE methods with lower PODs to achieve lower defect rates [22]. The actual defect rates can be estimated simply by dividing the recorded defects rates by PDs [49]. Various defect rates of the fabrication yards under study are calculated and summarised in Table 11 and plotted in Fig. 30 and Fig. 31. It can be seen that Yard 2 has both higher recorded and actual defect rates. Notice that incorporating PDs

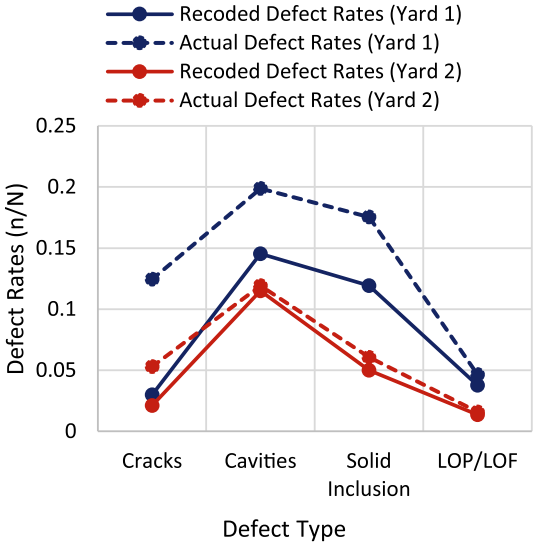

Fig. 30. Defect rates (number of defects divided by number of checkpoints): Recorded and Actual (Probability of Detection considered).

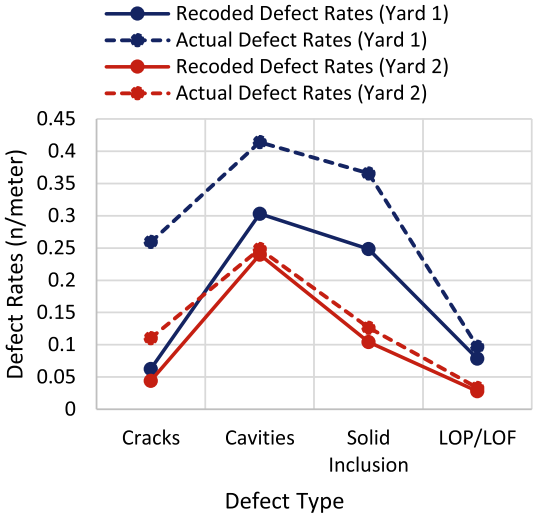

Fig. 31. Defect rates (number of defects divided by length of inspection): Recorded and Actual (Probability of Detection considered).

Table 11
Recorded and Estimated (POD considered) defect rates.

Manufacturer	Defect Type	Recorded			Estimated (POD considered)		
		Number	rate (n/N)	rate (n/m)	Number	rate (n/N)	rate (n/m)
Yard 1	Cracks	213	0.030	0.063	884	0.124	0.259
	Cavities	1033	0.146	0.303	1411	0.199	0.414
	Solid Inclusion	847	0.119	0.249	1246	0.175	0.366
	LOP/LOF	268	0.038	0.079	331	0.047	0.097
Yard 2	Cracks	64	0.021	0.044	160	0.053	0.110
	Cavities	348	0.115	0.240	360	0.119	0.248
	Solid Inclusion	151	0.050	0.104	183	0.061	0.126
	LOP/LOF	41	0.014	0.028	48	0.016	0.033

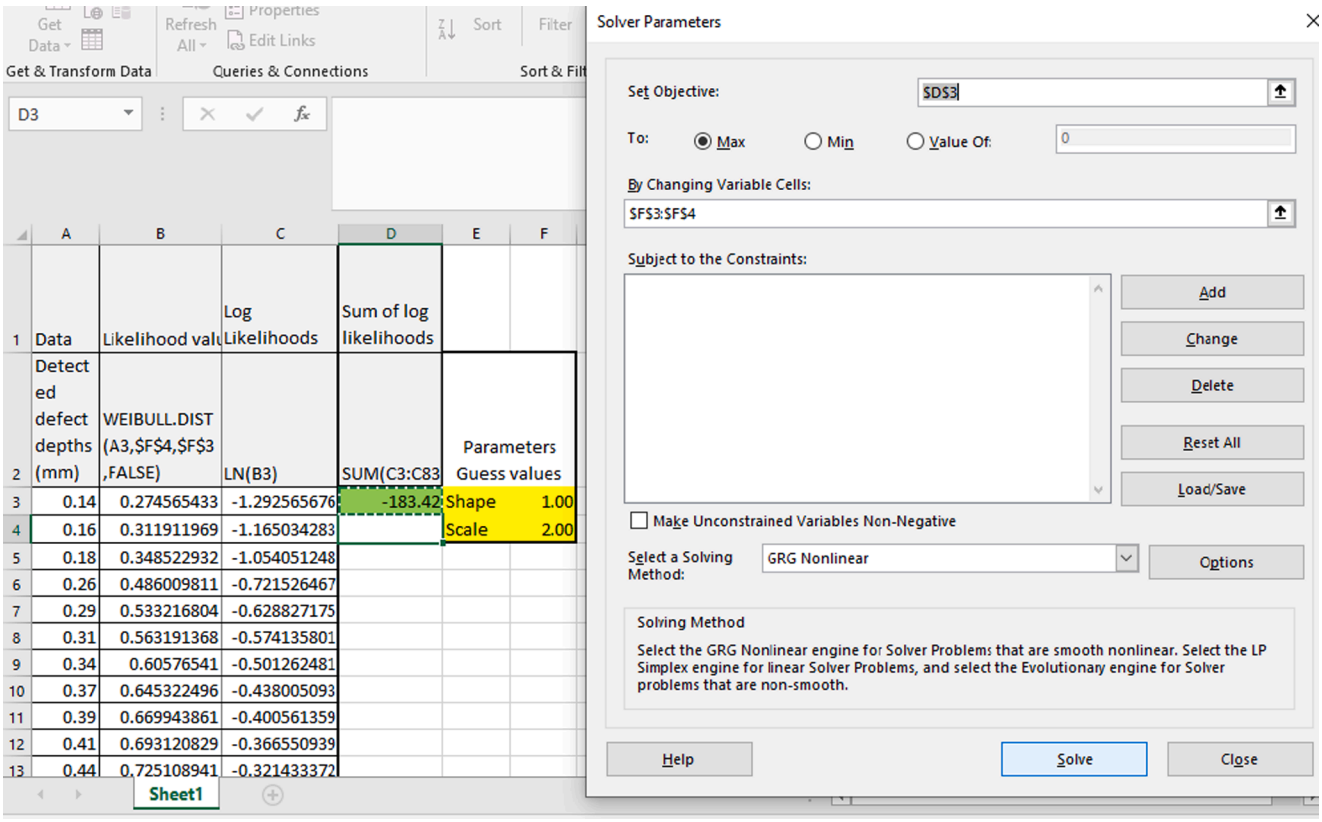

Fig. 32. MLE estimation of Weibull distribution in Excel.

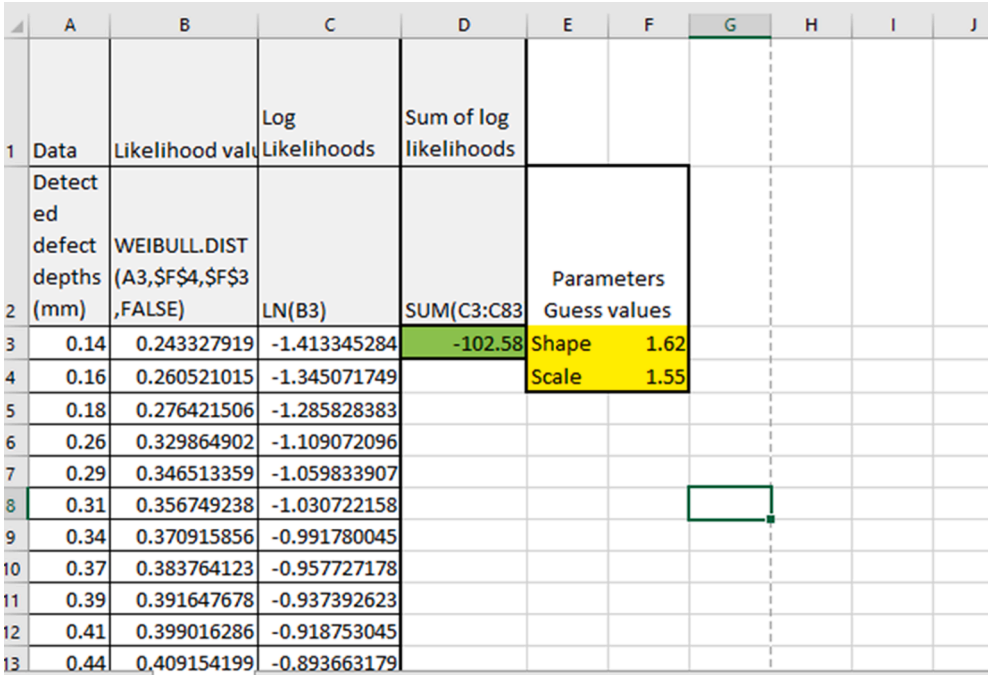

Fig. 33. Estimated Weibull distribution parameters.

significantly increases the difference between the defect rates of the two yards.

Overall, it is evident that compared to yard 1, yard 2 produces lower quality welds; bigger defect lengths and with higher frequency (higher defect rates). It also has worse weld quality control programme as far as NDE POD is concerned.

6. Concluding summary

Estimation of POD curves for NDE typically involves the manufacturing of a high number of specimens containing defects, followed by trial NDE and statistical analysis of the data based on the hit/miss approach. This is a time-consuming and costly procedure. In

addition to that, POD depends on variables such as human factors (operator) and test environment, resulting in a significant mismatch between those generated in the lab and those found in practice. Considering these parameters in the POD estimation is not always feasible, particularly when they vary during an inspection programme, for example in the quality control of welds in fabrication yards. The actual weld defect size distribution can be described by an exponential probability distribution function and the POD curves can be described by a cumulative distribution function with reasonable goodness-of-fit attributes.

In this paper, a method for estimating POD curves based on Bayesian theorem of conditional probability was presented. Then, the adequacy of predictions of the Bayesian Inference POD model were compared with a hit/miss-based model based on a pre-existing defect dataset from the NTIAC [2] data book and reported within a Health and Safety Executive report [5]. Overall the POD predicted by the Bayesian theorem was consistent with the more conventionally used hit/miss method.

The Bayesian model was used to estimate actual (detected + undetected) defect size distributions, defect rates and POD curves of various defect types for two shipbuilding fabrication yards. The findings are valuable inputs for estimating the fatigue reliability of newbuilt ships and offshore structures using a probabilistic ECA approach. Furthermore, it was found that one of the yards posses both lower welding quality; i.e. produces bigger and more frequent defects and lower weld quality control measures, as far as NDE POD is concerned.

In principle, the method can be easily built into a spread sheet and can be used by quality control personnel at the workshop. The results can be used, within a statistical quality control programme [55], to alert the QC team when the weld quality exceeds a predefined limit or the NDE capability of detection falls below a certain threshold. Subsequently, weld quality can be assessed with a more precise inspection method to confirm/reject welds based on quality criteria. Similarly, investigations can be done by, for example, a root cause analysis, to improve the NDE capabilities.

Declaration of Competing Interest

The authors declare that they have no known competing financial interests or personal relationships that could have appeared to influence the work reported in this paper.

Acknowledgements

This project has received funding from the European Union's Horizon 2020 research and innovation programme under grant agreement no. 74 5625 (ROMEO) ("Romeo Project" 2018). The dissemination of results herein reflects only the authors' views, and the European Commission is not responsible for any use that may be made of the information the paper contains.

Appendix

Defect depth data used in Proof of concept section

Detected defect depth (mm)					
0.14	0.57	0.95	1.33	1.96	2.96
0.16	0.59	0.98	1.36	2.45	2.98
0.18	0.62	1	1.38	2.47	3.03
0.26	0.64	1.02	1.45	2.62	3.21
0.29	0.67	1.05	1.48	2.67	3.8
0.31	0.7	1.08	1.51	2.7	4.53
0.34	0.72	1.1	1.53	2.73	
0.37	0.74	1.13	1.56	2.75	
0.39	0.77	1.15	1.58	2.78	
0.41	0.8	1.18	1.61	2.8	
0.44	0.82	1.2	1.63	2.83	
0.47	0.85	1.22	1.71	2.86	
0.49	0.87	1.25	1.74	2.87	
0.51	0.9	1.28	1.81	2.9	
0.54	0.92	1.3	1.94	2.93	

Undetected defect depths (mm)				
0.04	0.16	0.28	0.44	0.72
0.06	0.19	0.34	0.51	0.8
0.08	0.21	0.37	0.54	0.83
0.11	0.24	0.39	0.64	0.85
0.14	0.27	0.41	0.67	1.89

Data fitting example

In this example, for didactic purposes, estimation of the Weibull distribution parameters given in Table 7 and shown Fig. 9 and Fig. 10 are explained. The distribution parameters are estimated using MLE method in MS Excel and by following below steps:

1. The data detected defect depth sizes from the table in this appendix is inserted in the first column, A, ().
2. Likelihood values are estimated in column B using excel built-in Weibull distribution and guess parameter values in cell F3 and F4 (Fig. 32).
3. Loglikelihood values of column B are calculated in column C and using built-in LN function (Fig. 32).
4. Sum of Loglikelihood values are calculated in cell D3 by summing all cells in column C (Fig. 32).

5. Using excel solve add-in the distribution parameters are calculated by minimising cell D3 and by changing values in cells F3 and F4 (see Fig. 32 and Fig. 33).

References

[1] Fronthaler H, Croonen G, Biber J, Heber M, Rüther M. An online quality assessment framework for automated welding processes. Int J Adv Manuf Technol 2013;68(5-8):1655–64. https://doi.org/10.1007/s00170-013-4964-3.
[2] Rummel WD, Matzkanin GA. Nondestructive evaluation (NDE) capabilities data book (NTIAC: DB-97-02). NTIAC 625; 1997.
[3] British Standard. BS 7910:2019. London: Br Stand Institutions; 2019.
[4] Zhao W, Stacey A. Review of defect distributions for probabilistic structural integrity assessment. In: ASME 2002 21st International Conference on Offshore Mechanics and Arctic Engineering; 2002. p. 607–19.
[5] Georgiou GA. Probability of Detection (POD) curves: derivation, applications and limitations. Jacobi Consult Ltd Heal Saf Exec Res Rep 2006;454.
[6] Aker. Review of probabilistic inspection analysis methods. Health and Safety Executive; 1999.
[7] Kountouris IS, Baker MJ. Reliability of non-destructive examination of welded joints. Imperial College of Science and Technology Engineering Structures Laboratories. 1989.
[8] Becher PE, Hansen B. Statistical evaluation of defects in welds and design implications. Riso Danish Atomic energy commission research establishment; 1974.
[9] DNV. DNVGL-RP-C210-Probabilistic methods for planning of inspection for fatigue cracks in offshore structures; 2015.
[10] Jr AFG. Fundamentals of structural integrity: damage tolerant design and nondestructive evaluation. Hoboken: John Wiley & Sons; 2003.
[11] Shinozuka M. Relation of inspection findings to fatigue reliability; 1990.
[12] Hadley I. Improving safety with advanced fracture mechanics; 2019.
[13] Moan T, Song R. Implications of inspection updating on system fatigue reliability of offshore structures. J Offshore Mech Arct Eng 2000;122:173–80.
[14] Dnv. Fatigue reliability of old semi-submersibles. OTO Rep 2000;52.
[15] DNV, (DNV) Det Norske Veritas. Structural reliability analysis of marine structures. Det Norske Veritas; 1992.
[16] ASM. ASM Handbook Vol. 17 - Nondestructive Evaluation and Quality Control. ASM Int Met Park OH 1608; 1992.
[17] da Silva RR, de Padu GX. Nondestructive inspection reliability: state of the art. Nondestruct Test Methods New Appl 2012. https://doi.org/10.5772/37112.
[18] Førli O. Guidelines for development of NDE acceptance criteria. Nordtest 1999.
[19] Habibzadeh Boukani H, Viens M, Tahan S-A, Gagnon M. Case study on the integrity and nondestructive inspection of flux-cored arc welded joints of Francis turbine runners. Int J Adv Manuf Technol 2018;98(5-8):2201–11. https://doi.org/10.1007/s00170-018-2139-y.
[20] Schneider CRA, Sanderson RM, Carpentier C, et al. Estimation of probability of detection curves based on theoretical simulation of the inspection process. In: 51st Annu Conf Br Inst Non-Destructive Test 2012, NDT 2012:393–404.
[21] Schmerr LW. Fundamentals of ultrasonic nondestructive evaluation a modeling approach second edition; 2016.
[22] Amirafshari P, Barltrop N, Bharadwaj U, Wright M, Oterkus S. A review of nondestructive examination methods for new-building ships undergoing classification society survey. J Sh Prod Des 2018;34(01):9–19.
[23] Aldrin JC, Annis C, Sabbagh HA, Lindgren EA. Best practices for evaluating the capability of nondestructive evaluation (NDE) and structural health monitoring (SHM) techniques for damage characterization. AIP Conference Proceedings. 2016.
[24] Koh YM, Meeker WQ. Quantile POD for nondestructive evaluation with hit–miss data. Res. Nondestruct. Eval. 2019;30:89–111.
[25] Astm. Standard practice for probability of detection analysis for hit / miss data E2862. ASTM Int 2018;i:1–14.
[26] Matzkanin GA, Yolken HT. Probability of detection (POD) for Nondestructive Evaluation (NDE); 2001.
[27] Subair M, Akbar S, Rajagopal P. Probability of Detection (PoD) curves based on Weibull statistics. J Nondestruct Eval 2018;37:1–13. https://doi.org/10.1007/s10921-018-0468-2.
[28] Kountouris IS, Baker MJ. Defect assessment: analysis of the dimensions of defects detected by ultrasonic inspection in an offshore structure. Imperial College of Science and Technology Engineering Structures Laboratories. 1989.
[29] Kountouris IS, Baker MJ. Defect assessment: analysis of the dimensions of defects detected by magnetic particle inspection in an offshore structure. Imperial College of Science and Technology Engineering Structures Laboratories. 1989.
[30] Baker, Kountouris, Ohmart. Weld defects in an offshore structure, a detailed study. In: Int. Conf. On Behavior of Offshore Structures; 1988.
[31] Visser W. POD/POS curves for non-destructive examination. HSE Books; 2002.
[32] Dufresne J. Probabilistic application of fracture mechanics; 1981.
[33] Rentala VK, Mylavarapu P, Gautam JP. Issues in estimating probability of detection of NDT techniques – A model assisted approach. Ultrasonics 2018;87:59–70. https://doi.org/10.1016/j.ultras.2018.02.012.
[34] Schubert Kabban CM, Greenwell BM, DeSimio MP, Derriso MM. The probability of detection for structural health monitoring systems: repeated measures data. Struct Heal Monit 2015;14(3):252–64. https://doi.org/10.1177/1475921714566530.
[35] Hellier C, Shakinovsky M. Handbook of nondestructive evaluation. McGraw-Hill New York; 2001.
[36] Sause MGR, Linscheid FF, Wiehler M. An experimentally accessible probability of detection model for acoustic emission measurements. J Nondestruct Eval 2018;37:1–12. https://doi.org/10.1007/s10921-018-0474-4.
[37] Extende. CIVA Software; 2020. http://www.extende.com/civa-in-a-few-words. Accessed 1 Apr 2020.
[38] Extende. CIVA aim; 2020. http://www.extende.com/what-civa-brings-to-ndt. Accessed 1 Apr 2020.
[39] Walker T, Stevens A, Cool T. Use of monte-carlo methods to derive quantitative probability of defect detection data. Nucl Futur 2009;5:13–21.
[40] Moan T, Wei Z, Vardal OT. Initial crack depth and POD data based on underwater inspection of fixed steel platforms. Struct Saf Reliab ICOSSAR'01 2001; 2001.
[41] Sata A, Ravi B. Bayesian inference-based investment-casting defect analysis system for industrial application. Int J Adv Manuf Technol 2017;90(9-12):3301–15. https://doi.org/10.1007/s00170-016-9614-0.
[42] Syed Akbar Ali MS, Kumar A, Rao PB, Tammana J, Balasubramaniam K, Rajagopal P. Bayesian synthesis for simulation-based generation of probability of detection (PoD) curves. Ultrasonics 2018;84:210–22. https://doi.org/10.1016/j.ultras.2017.11.004.
[43] Ang 1930- AH-S (Alfredo H-S, Tang (joint author). WH, Ang 1930-. Probability concepts in engineering planning and design. AH-S. Probability concepts in engineering : emphasis on applications in civil & environmental engineering / Alfredo H-S. Ang, Wilson H. Tang. xiii, p. 406.
[44] Marin J-M, Robert C. Bayesian core: a practical approach to computational Bayesian statistics. Springer Science & Business Media; 2007.
[45] Williams S, Mudge PJ. Statistical aspects of defect evaluation using ultrasonics. NDT Int 1985;18(3):123–31.
[46] Rogerson JH, Wong WK. Weld defect distributions in offshore structures and their influence on structural reliability. Soc Pet Eng AIME, Pap;(United States) 1982:2.
[47] Karadeniz H. Stochastic analysis of offshore steel structures: an analytical appraisal. Springer Science & Business Media; 2012.
[48] Burdekin FM, Towned PH. Reliability aspects of fracture on stress concentration regions in offshore structures, integrity of offshore structures. In: 2nd Int. In: Symp., Glasgow.
[49] Moan T, Vårdal OT, Hellevig N-C, Skjoldli K. In-service observations of cracks in north sea jackets. A study on initial crack depth and POD values. In: Proceedings of the international conference on offshore mechanics and arctic engineering; 1997. p. 189–98.
[50] Gelman A, Stern HS, Carlin JB, et al. Bayesian data analysis. Chapman and Hall/CRC; 2013.
[51] Sørensen JD, Toft HS. Probabilistic design of wind turbines. Energies 2010;3(2):241–57. https://doi.org/10.3390/en3020241.
[52] Celeux G, Persoz M, Wandji JN, Perrot F. Using Markov chain Monte Carlo methods to solve full Bayesian modeling of PWR vessel flaw distributions. Reliab Eng Syst Saf 1999;66(3):243–52. https://doi.org/10.1016/S0951-8320(99)00041-1.
[53] Forbes C, Evans M, Hastings N, Peacock B. Statistical distributions. 4th ed. New Jersey: John Wiley&Sons Inc; 2011.
[54] Amirafshari P, Stacey A. Review of available probabilistic models of the crack growth parameters in the Paris equation. In: OMAE2019-961. OMAE; 2019.
[55] Amirafshari P, Brennan F, Kolios A. A fracture mechanics framework for optimising design and inspection of offshore wind turbine support structures against fatigue failure. Wind Energy Sci 2021;6:677–99. https://doi.org/10.5194/wes-6-677-2021.
[56] Amirafshari P. Optimising Non-destructive Examination of newbuilding ship hull structures by developing a data-centric risk and reliability framework based on fracture mechanics. University of Strathclyde; 2019.
[57] Garza J, Millwater H. Sensitivity of the probability of failure to probability of detection curve regions. Int J Press Vessel Pip 2016;141:26–39. https://doi.org/10.1016/j.ijpvp.2016.03.012.
[58] Lassen T, Recho N. Fatigue life analyses of welded structures: flaws. John Wiley & Sons; 2013.
[59] Marshall W. An assessment of the integrity of PWR pressure vessels; 1982.
[60] Bokalrud T, Karlsen A. Probabilistic fracture mechanics evaluation of fatigue failure from weld defects in butt welded joints. Proc. Conf. on fitness for purpose validation of welded constructions. 1982.
[61] Amirafshari P, Barltrop N, Bharadwaj U, et al. Non-destructive examination of new-building ships – current state, gaps, needs, and recommendations. Maritime & Naval Test Development Symposium. 2017.
[62] Marcello Consonni CFW. Repair rates in welded construction - an analysis of industry trends. Weld Cut 2012:33–5.
[63] Jonsson B, Dobmann G, Hobbacher AF, et al. IIW guidelines on weld quality in relationship to fatigue strength. Cham: Springer International Publishing; 2016.
[64] Amirafshari P, Barltrop N, Wright M, Kolios A. Weld defect frequency, size statistics and probabilistic models for ship structures. Int J Fatigue 2021;145:106069. https://doi.org/10.1016/j.ijfatigue.2020.106069.